# Role of oxygen vacancy defect states in the *n*-type conduction of $\beta$-Ga$_2$O$_3$

Zoltán Hajnal,[a),b)] József Miró, Gábor Kiss, Ferenc Réti, Péter Deák, Roy C. Herndon, and J. Michael Kuperberg

*Center for Hungarian-American Environmental Research, Studies and Exchanges,*
*Department of Atomic Physics, Technical University of Budapest, Budafoki út 8, H-1111 Hungary*

Based on semiempirical quantum-chemical calculations, the electronic band structure of $\beta$-Ga$_2$O$_3$ is presented and the formation and properties of oxygen vacancies are analyzed. The equilibrium geometries and formation energies of neutral and doubly ionized vacancies were calculated. Using the calculated donor level positions of the vacancies, the high temperature *n*-type conduction is explained. The vacancy concentration is obtained by fitting to the experimental resistivity and electron mobility. © *1999 American Institute of Physics.* [S0021-8979(99)03318-6]

## I. INTRODUCTION

The developments of the last decade in microelectronics allow, among other things, the automatic monitoring and control of chemical processes. Operations of this kind are generally based on three units: (a) the monitoring unit (sensor) (b) the central processing unit (CPU), and (c) the controlling unit (actuator). For example, a sensor unit in automobiles may measure the exhaust gas composition, the CPU optimizes and the actuator controls the injected fuel composition for maximum performance at minimum consumption and emission. The closer the sensor is to the engine, the more effective the system. This means, however, extreme chemical and thermal conditions, which the sensor must endure.

Many semiconducting oxides show characteristic changes in conductivity when exposed to certain oxidizing or reducing atmospheres. This feature makes them candidates for sensor materials, but their resistance and signal stability is poor in most of the cases. An exception is the chemically and thermally extremely stable, oxygen sensing $\beta$-Ga$_2$O$_3$.

Ga$_2$O$_3$ shows polymorphism, but at high temperatures only its $\beta$ form[1] is stable, and this is preserved upon cooling. Its melting point is around 1900 °C, and it does not dissolve even in concentrated acids. Its conductivity ($\sigma$) at high temperatures is proportional to the $-1/4$-th power of the oxygen partial pressure[2] in the surrounding gas:

$$\sigma \sim P_{O_2}^{-1/4} e^{-\frac{E_A}{k_B T}}, \tag{1}$$

with an activation energy ($E_A$) of $\sim$2 eV at 950 °C.

The electronic properties of single-crystalline $\beta$-Ga$_2$O$_3$ are varying from insulator to conductor, depending on the circumstances of preparation (substrate temperature, ambient composition, post-processing).[3] In sensor applications for reducing gases, the effect of adsorbed molecules on the polycrystalline grain walls is used,[4] while oxygen sensing at high temperatures ($>$600 °C) can be related to the thermal equilibrium of the O vacancy concentration with the partial pressure of O$_2$ of the atmosphere.[5]

The optical band gap of the single-crystalline material has been measured to be 4.2–4.9 eV.[6–9] The reason of this relative uncertainty might be the anisotropy of the monoclinic material, and/or the difference in preparation. The gap values $\sim$4.4 eV, measured for polycrystals,[10] are also in the above mentioned energy interval.

Considering the coordinational difference of the lattice sites in $\beta$-Ga$_2$O$_3$ (e.g., four-fold and six-fold coordinated Ga sites), ions at different sites can have very different binding energies in the crystal.[6,11] A further difference between the Ga atoms is shown in band-structure calculations[11] based on the Extended Hückel Theory (EHT): simplified structural models give rise to a 60% Ga 4*s* contribution to the lowest lying conduction band, that comes almost entirely from the octahedral (six-fold coordinated) Ga atoms. Except for these results, the whole electronic band structure of $\beta$-Ga$_2$O$_3$ has not been investigated, neither theoretically nor experimentally.

The band-to-band transitions, observed in optical absorption measurements, show similar spread in results in the case of different research groups and samples. Photoconductivity experiments, aimed at exploring the gap states, raised reproduction problems,[6] with the only common observation that the conductivity response starts at $\sim$3.3 eV and has a peak around the band gap energy. More recent electron energy loss spectroscopy (EELS) studies[12] have also found a gap state at this energy.

In spite of the fact that the equilibration of O vacancies with the O$_2$ of the ambient gas is commonly accepted as the principal mechanism of oxygen sensing, formation and migration of these vacancies, and their effects on the electronic properties have not yet been theoretically investigated.

Changes in the conductivity of $\beta$-Ga$_2$O$_3$ are observed to be primarily related to changes in the carrier density.[3] This density change, in turn, is caused by deviations of the O content of the bulk material from the stoichiometric ratio.[13] To establish a theoretical background to these observations, we have studied the equilibrium geometry and electronic

[a)] Also at: Research Institute for Technical Physics and Materials Science, P.O.B. 49, Budapest, H-1525 Hungary.
[b)] Corresponding address: Theoretische Physik, Universität-GH Paderborn, D-33095 Germany; electronic mail: hajnal@scientist.com
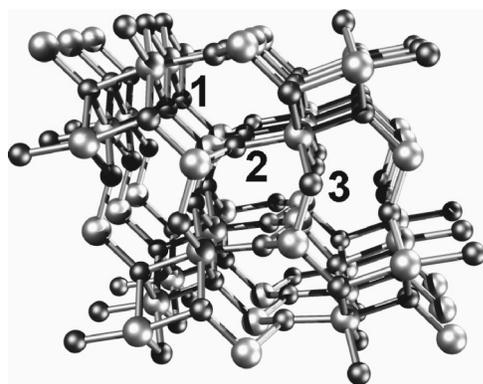
FIG. 1. $1 \times a_0$, $3 \times b_0$, $2 \times c_0$ supercell of $\beta$-$Ga_2O_3$. Ga atoms are the larger light shaded, the O atoms the smaller dark shaded ones. The numbers mark the three different O (vacancy) sites.

structure of $V_O$ at all three possible lattice sites. In Sec. II we briefly recall the crystal structure information on $\beta$-$Ga_2O_3$, then describe the supercell model we used in our calculations. Next, we consider the applicable methods and our choice of the PM3 semiempirical quantum-chemical Hamiltonian. In Sec. III, we analyze the relaxation of the Ga neighbors of the O vacancies. The total energies of the supercells containing the defects are then used to calculate and sort the formation energies of the six cases under consideration (that is the three different O vacancy sites, all three in neutral and doubly positively charged states). Also, the electronic structure of the defect states is analyzed. This is used to model the *n*-type conductivity. Finally, the defect density is estimated by fitting the model parameter to the observed temperature dependence of a given polycrystalline sample. A summary of the presented results is given in Sec. IV.

## II. COMPUTATION

### A. Structure of $\beta$-$Ga_2O_3$

The space group of the crystal structure of $\beta$-$Ga_2O_3$ is $C_{2/m}$, with a base centered monoclinic unit cell containing 8 Ga and 12 O atoms[1] (see Fig. 1). Half of the Ga atoms has six O neighbors in a distorted octahedral arrangement, the other half is tetrahedrally coordinated. The numbers show the three inequivalent positions of the O atoms in the crystal: (1) has four Ga neighbors tetrahedrally arranged, (2) lies in the plane of a Ga triangle, (3) is out of plane of a Ga triangle. N.b., the primitive unit cell of this structure contains only half as many atoms as the conventional one, and the primitive translation vectors $(a', b', c')$ can be constructed from $a_0$, $b_0$, $c_0$ as follows:

$$a' = \frac{a_0 - b_0}{2}, \quad b' = \frac{a_0 + b_0}{2}, \quad c' = c_0. \quad (2)$$

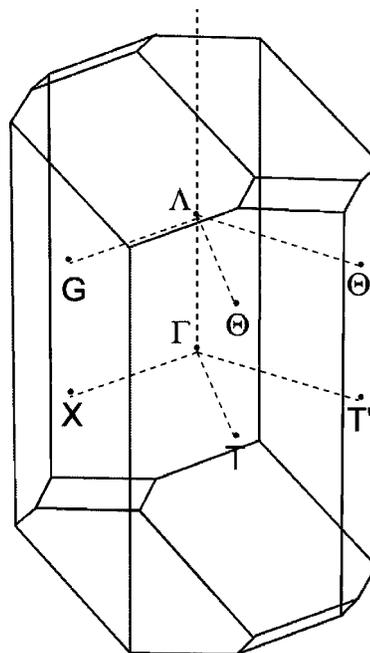The Brillouin zone (BZ), defined by these primitive translations is depicted on Fig. 2.



FIG. 2. Brillouin zone of $\beta$-$Ga_2O_3$. The *k* points that overlap in the $\Gamma$ point of the 1-3-2 supercell are marked with different letters.

### B. Applied computational methods

We have used the cyclic cluster model (CCM) for the crystalline environment around a defect in $Ga_2O_3$. In this method, a multiple of the unit cell is taken into account, and cyclic boundary conditions are applied.

The CCM has been developed to be used in conjunction with linear combination of atomic orbitals (LCAO) electronic structure calculations.[14] The electronic interactions are defined to be restricted to the Wigner–Seitz cell. The choice of the supercell defines a reduced BZ. Since our CCM calculations take only the $\Gamma$ point of the reduced BZ into account, we have to choose the supercell so that the *k* points that are folded into the $\Gamma$ represent a so-called special *k*-point set.[15] The choice of the supercell vectors,

$$a = a_0, \quad b = 3 \times b_0, \quad c = 2 \times c_0 \quad (3)$$

results in a set of special *k* points, that satisfies the Chadi–Cohen criteria[15] up the ninth neighbor shell. The 120 atom supercell is shown in Fig. 1, the *k*-point set in Fig. 2. This supercell is the best one in the size range that is still of reasonable computational demand. Our model for the crystal structure uses the x-ray diffraction data, due to Geller.[1]

There exist already localized basis implementations of the *first principles* local density approximation (LDA) of density functional theory (DFT) applying CCM,[16] but the size of the system (120 atoms) only allowed us to use it for the defect free cell.

The minimal basis semiempirical Hartree–Fock methods appear to be the optimal choice for energy minimization and electronic structure calculations. The PM3 parametrization of the NDDO quantum-chemical Hamiltonian[17] have already been proven to be useful in the analysis of point defects in apolar semiconductors.[14] Because of its self-consistent treatment of the electronic structure, we expect it to describe

qualitative trends also in a system where considerable charge transfer occurs due to polar bonds. Examples for such systems are O containing Si surface structures[18] and silicon suboxides.[19] Since parametrization of the method was focusing on binding energies and molecular geometries,[17] semi-quantitative prediction of vacancy formation energies and relaxation geometries will be possible.

## III. RESULTS AND DISCUSSIONS

### A. Electronic structure of $\beta$-Ga$_2$O$_3$

Regarding the ionicity of the bonds, a key property for the estimation of vacancy formation energies, $\beta$-Ga$_2$O$_3$ is a border-line case. There is, unfortunately, no experimental data for this property, and the basic approximations applied in chemistry predict a wide range of charge transfer values. Using the difference in Pauling electronegativity, 1.6, the Ga–O bond is 60% ionic, that is the charge transfer to the O atoms is 1.2$e$. The Pauling data are derived from diatomic (i.e., multiple bonded) molecules, thus they are expected to overestimate ionicity in more complex systems. The other extreme is provided by the Sanderson-type[20] partial charge, which is 0.19 for Ga$_2$O$_3$. For comparison, in the case of SiO$_2$, the Pauling charge transfer would be 1.0$e$, the Sanderson partial charge 0.25. This tells us to handle these results very carefully, since even the predicted trends are opposite in the two methods. A *first principles* LDA calculation[16] on the perfect cell at the experimental geometry, with a small basis set (six contracted Gaussians for all $s$ and $p$ orbitals) resulted in a charge transfer of 0.46$e$ for the fourfold coordinated O atoms (marked 1 in Fig. 1), and 0.27$e$ and 0.34$e$ for the threefold coordinated ones (Fig. 1: 2 and 3, respectively). Due to the known overbinding effect in LDA, the calculated binding energy, −4.02 eV/bond is significantly exceeding the experimental value of −2.46 eV/bond.

Using the PM3 semiempirical method, we have minimized the total energy of the 120 atom 1-3-2 supercell with respect to the cell dimensions. The symmetry relations of the $\beta$-Ga$_2$O$_3$ crystal have been applied. The optimum lattice vectors we found to be 6% shorter than the experimental value, and the binding energy was −3.04 eV/bond. This is a more realistic result, than that of the LDA, but is still stronger than the experimental bond strength. The reason for this, and the shorter bonds as well, is likely to be the overestimation of charge transfer, 1.45$e$ for the four-fold, and 1.34$e$ for the three-fold coordinated O atoms. The band gap, calculated from the total energy of the supercell in ground and excited state, is 5.58 eV. The deviation from the experimental values of 4.2–4.9 eV is mainly due to the finite model, and also because of the overestimated ionicity of the bonds. The calculated band structure is shown in Fig. 3. The energy values at the marked $k$ points (same as in Fig. 2) are simply connected with straight lines. This is the band-structure calculation for $\beta$-Ga$_2$O$_3$ with an SCF electronic structure method.

Detailed analysis of the wave functions confirms the prediction from EHT calculations[11] that the conduction band edge has 64% contribution from Ga 4$s$ states. However, we do not find considerable difference between the contributions from the tetrahedral and the octahedral Ga atoms. Thus, the
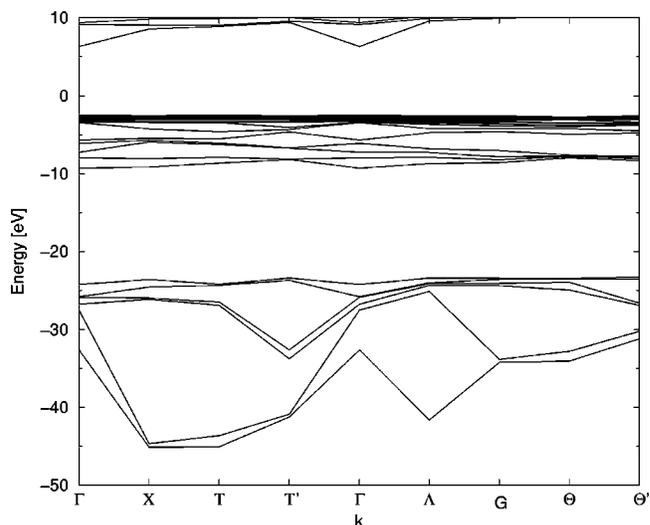


FIG. 3. Band structure of $\beta$-Ga$_2$O$_3$, between the special $k$ points of the 1-3-2 supercell.

conduction band edge states can be treated as extended $ss\sigma$ states of the 1D chain of Ga atoms in the $b_0$ lattice direction. This anisotropy explains the observed polarization dependence in optical absorption as well as the anisotropy in the conductivity.[3,9] The valence band edge states, on the other hand, are arising from the nonbonding electron pairs of the three-fold coordinated O atoms, with almost negligible dispersion. The fundamental optical transitions are then the excitations between these two types of states. The nonbonding oxygen states, due to their weak interactions with each other, might explain the experimentally observed exciton self-trapping.[21]

The higher energy part of the valence band consists entirely of weakly interacting O 2$p$ orbitals, while the lower energy band contains the Ga 4$s$–O 2$p$ bonding states.

### B. Oxygen vacancies in $\beta$-Ga$_2$O$_3$

The vacancy formation energies have been calculated from the reaction

$$Ga_2O_3 \rightarrow Ga_2O_3 : V_O + \tfrac{1}{2}O_2. \tag{4}$$

It is generally assumed that vacancies in ionic compounds are formed in their doubly positive (absolute) charge state. The formation in this case is described by the reaction

$$Ga_2O_3 \rightarrow Ga_2O_3 : V_O^{++} + \tfrac{1}{2}O_2 + 2e^-, \tag{5}$$
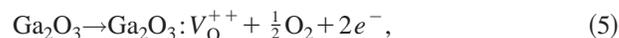
where the electrons are moved to the vacuum energy level (0 eV). Table I shows the estimated formation energies of the neutral ($E_{vac}$) and the doubly charged ($E_{vac}^{++}$) vacancies. They have been calculated using the PM3 total energies of the defect and the perfect supercell. Since the CCM does not take long range Coulomb interactions into account, the presented values can only be used to compare formation energies of defects in the same charge state (i.e., in column $E_{vac}$ or $E_{vac}^{++}$ of Table I). The structural relaxation was allowed up to the second nearest neighbor shell, total energies have been converged to within 0.001 eV/atom.

TABLE I. Formation energies and donor levels of the O vacancies in $\beta$-Ga$_2$O$_3$.

| Sign[a] | Coordination | $E_{\text{vac}}$ (eV) | $E_{\text{vac}}^{++}$ (eV) | $E_{\text{don}}$[b] |
|---------|--------------|-----------------------|----------------------------|---------------------|
| 1 | 4 | 5.3 | 4.3 | 4.3 |
| 2 | 3 | 4.0 | 6.1 | 2.8 |
| 3 | 3 | 6.3 | 5.2 | 4.2 |

[a]See Fig. 1
[b]With respect to the valance band edge.

The neutral vacancies give rise to doubly occupied donor levels in the gap. The energy values of these are shown in the column $E_{\text{don}}$ of Table I.

The relaxation of the neighboring Ga atoms is different in the case of different sites: The first vacancy (fourfold coordinated, number 1 in Fig. 1) has three Ga neighbors that are octahedrally, and one that is tetrahedrally coordinated. The former ones relax 0.07 Å outwards from the vacancy site, while the latter one is relaxing 0.2 Å inwards. The donor state is localized on this atom, so that the Ga 4$s$ and 4$p$ contribution is ~70% with an $s/p$ ratio of 2.5. The $p$ contribution makes this state point towards the vacancy site.

Two tetrahedral Ga neighbors of the second vacancy (threefold coordinated, number 2 in Fig. 1) are relaxing 0.3 Å inwards and form a weak $ss\sigma$ bond. The octahedral Ga relaxes 0.07 Å outwards. The above mentioned doubly occupied bonding state has an energy level in the forbidden gap. In the neutral state, this vacancy seems to be energetically favorable, but the gap state lies so deep in energy, that it can not be considered as a donor even at very high temperatures. It might serve as hole trap, though. It is also likely to be the gap state giving rise to the photoconductivity response,[6] and also seen in EELS spectra.[12]

The third (out of Ga triangle, number 3 in Fig. 1) vacancy has the highest formation energy in its neutral state. The relaxation of its two octahedral Ga neighbors is outwards, and the tetrahedral relaxes inwards. This is similar to case of the first (fourfold coordinated vacancy) as is the donor state, localized on the tetrahedrally coordinated, inward relaxing Ga atom.

## C. Model for the *n*-type conduction

In the previous section, we have shown that oxygen vacancies are functioning as donors, thus explaining the high temperature *n*-type conduction in $\beta$-Ga$_2$O$_3$. Now, it is possible to construct an approximative expression for the conduction electron density ($n_c$) as a function of temperature, supposing the O vacancy concentration ($N_v$) to be constant, and the lowest energy neutral, and lowest energy doubly charged vacancies to be in thermal equilibrium:

$$n_c \approx N_v [ e^{-\Delta E/k_B T} e^{-E_{d1}/2k_B T} + (1 - e^{-\Delta E/k_B T}) e^{-E_{d2}/2k_B T} ]. \tag{6}$$

Here, $\Delta E$ is the formation energy difference (1.3 eV) in the neutral state of vacancies 1 and 2, $E_{d1}$ and $E_{d2}$ are the donor level ionization energies (1.2 and 2.5 eV, respectively).
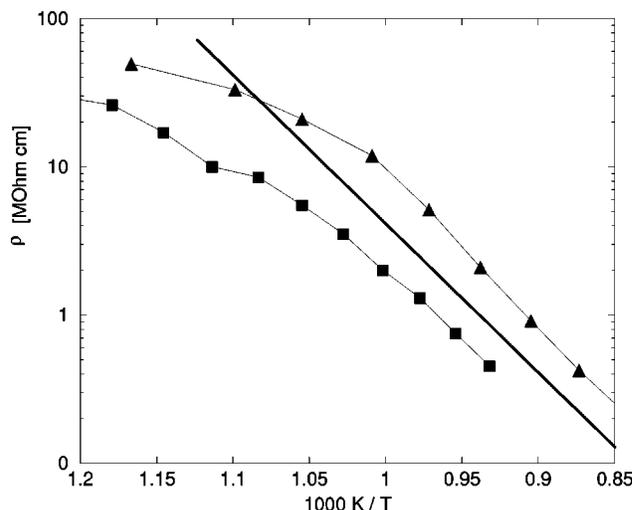


FIG. 4. Arrhenius plot of the resistivity of $\beta$-Ga$_2$O$_3$. Square points: polycrystalline sample in pure N$_2$ atmosphere. Triangles: polycrystalline sample in vacuum. Thick solid line: calculated assuming a $V_O$ density of 5.0 $\times 10^{18}$ cm$^{-3}$.

Conductivity and Hall measurements on $\beta$-Ga$_2$O$_3$ have shown[22] that the conduction is purely electronic, and that the mobility in the single- as well as the polycrystalline phases can be described by the relation

$$\mu \sim e^{-0.6 \text{ eV}/k_B T}, \tag{7}$$

and the value of the mobility is 5 cm$^2$ V$^{-1}$ s$^{-1}$ at 1000 °C. Using Eq. (6) for the calculation of carrier density and Eq. (7) for the carrier mobility, one can express the resistivity as

$$\rho = \frac{1}{\sigma} = \frac{1}{e n_c \mu} \tag{8}$$

with only one constant, the vacancy concentration remaining undefined. Figure 4 shows the Arrhenius plot of the resistivity of polycrystalline $\beta$-Ga$_2$O$_3$ samples in pure $N_2$ atmosphere and in vacuum (squares and triangles, respectively). The solid line shows the calculated resistivity, using Eq. (8). The assumed vacancy concentration is $N_v = 5.0 \times 10^{18}$ cm$^{-3}$. A good agreement for the higher temperature region is achieved. The difference at lower temperatures (under ~900 K) arises probably from the contribution of other conductivity mechanisms.

## IV. SUMMARY

The electronic band structure of the perfect $\beta$-Ga$_2$O$_3$ has been calculated in a 120 atom CCM cell using the PM3 semiempirical Hamiltonian. With the same Hamiltonian and assuming up to second nearest neighbor relaxation, the total energy of supercells containing an oxygen vacancy have been minimized with respect to atomic coordinates, applying no symmetry restrictions. It is generally observed that the octahedrally coordinated Ga atoms relax only very little away from the vacancy, while the tetrahedral ones relax considerably towards the vacancy center. Neutral and doubly positively charged states have been found to be stable, and formation energies of these have been derived.

The lowest formation energy belongs to one of the three-fold coordinated vacancies in the neutral, and to the fourfold coordinated O vacancy in its doubly positive state. High temperature *n*-type conduction in $\beta$-$Ga_2O_3$ is explained on the basis of the thermal equilibrium of these two vacancy sites. In a simple model, involving only the two lowest energy vacancy sites, and by fitting only a single parameter to reproduce experimental resistivity values, the oxygen vacancy concentration is estimated to be $\sim 5.0 \times 10^{18} cm^{-3}$, in oxygen-free atmosphere.

The characteristic donor state is essentially a combination of the localized Ga $4s$ and $4p$ states, with an *s/p* ratio of 2.5.

A deep state at $\sim 2.8$ eV from the valance band edge is identified as a $(ss\sigma)$ Ga–Ga bond, the product of the relaxation of the minimum energy neutral O vacancy.

## ACKNOWLEDGMENTS

[1] S. Geller, J. Chem. Phys. **33**, 676 (1960).

[2] K. Bernhardt, M. Fleischer, and H. Meixner, Siemens Components **30**, 35 (1995).

[3] M. Fleischer and H. Meixner, J. Mater. Sci. Lett. **11**, 1728 (1992).

[4] M. Fleischer, L. Höllbauer, and H. Meixner, Sens. Actuators B **18**, 119 (1994).

[5] M. Fleischer, J. Giber, and H. Meixner, Appl. Phys. A: Solids Surf. **54**, 560 (1992).

[6] H. H. Tippins, Phys. Rev. A **140**, 316 (1965).

[7] T. Matsumoto, M. Aoki, A. Kinoshita, and T. Aono, Jpn. J. Appl. Phys., Part 1 **13**, 1578 (1974).

[8] H.-G. Kim and W.-T. Kim, J. Appl. Phys. **62**, 2000 (1987).

[9] N. Ueda, H. Hosono, R. Waseda, and H. Kawazoe, Appl. Phys. Lett. **71**, 933 (1997).

[10] M. Passlak, E. F. Schubert, W. S. Hobson, M. Hong, N. Moriya, S. N. G. Chu, K. Konstadinidis, J. P. Mannaerts, M. L. Schnoes, and G. J. Zydzik, J. Appl. Phys. **77**, 686 (1995).

[11] L. Binet, D. Gourier, and C. Minot, J. Solid State Chem. **113**, 420 (1994).

[12] G. Schmitz, P. Gassmann, and R. Franchy, J. Appl. Phys. **83**, 2533 (1998).

[13] F. Bozon-Venduraz, C. Potvin, and G. Pannetier, J. Chim. Phys. **67**, 1608 (1970).

[14] P. Deák, L. R. Snyder, and J. W. Corbett, Phys. Rev. B **45**, 11612 (1992).

[15] D. J. Chadi and M. L. Cohen, Phys. Rev. B **8**, 5747 (1973).

[16] J. Miró, P. Deák, C. P. Ewels, and R. Jones, J. Phys.: Condens. Matter **9**, 9555 (1997).

[17] J. J. P. Stewart, J. Comput. Chem. **10**, 209 (1989).

[18] P. Deák, Z. Hajnal, and J. Miró, Thin Solid Films **276**, 290 (1998).

[19] Z. Hajnal, P. Deák, Th. Köhler, R. Kaschner, and Th. Frauenheim, Solid State Commun. **108**, 93 (1998).

[20] R. T. Sanderson, *Chemical Bonds and Bond Energy,* 2nd ed. (Academic, New York, 1976).

[21] A. I. Kuznetsov, V. N. Abramov, and T. V. Uibo, Opt. Spectrosc. **58**, 368 (1985).

[22] M. Fleischer and H. Meixner, J. Appl. Phys. **74**, 300 (1993).